Efficient computation of almost invisible inputs for linear input redundant systems

Jérémie Kreiss, Mohammad Fahim Shakib, Marc Jungers

▶ **To cite this version:**

Jérémie Kreiss, Mohammad Fahim Shakib, Marc Jungers. Efficient computation of almost invisible inputs for linear input redundant systems. 23rd European Control Conference, ECC 2025, Jun 2025, Thessaloniki, Greece. ⟨hal-05097911⟩

HAL Id: hal-05097911

https://hal.science/hal-05097911v1

Submitted on 4 Jun 2025

HAL is a multi-disciplinary open access archive for the deposit and dissemination of scientific research documents, whether they are published or not. The documents may come from teaching and research institutions in France or abroad, or from public or private research centers.

L'archive ouverte pluridisciplinaire **HAL**, est destinée au dépôt et à la diffusion de documents scientifiques de niveau recherche, publiés ou non, émanant des établissements d'enseignement et de recherche français ou étrangers, des laboratoires publics ou privés.

HAL Authorization

Efficient computation of almost invisible inputs for linear input redundant systems

J. Kreiss, M.F. Shakib, and M. Jungers

Abstract— **Input redundant systems have more inputs than needed to control the output and offer advantages such as fault tolerance and improved performance. However, identifying such redundant inputs in high-dimensional systems can be computationally intensive and is prone to inaccuracies. This article proposes an approach that uses model reduction by balanced truncation to simplify input redundancy analysis. By reducing the system order, we identify "invisible inputs" for the reduced-order model and design a reduced order state feedback mechanism to decouple them from the "visible inputs." Then, error bounds from balanced truncation provide guarantees for applying this decoupling to the original system, as a feedforward input. The approach offers significant computational savings, as demonstrated in numerical examples.**

I. Introduction

Many engineering and control systems are designed with more inputs than strictly necessary to control the system output [1], resulting in what is known as an *input redundant* (IR) system [2]. This redundancy offers several advantages, such as failure resilience, improved performance, and improved managing of the state-of-health [1], [3], [4], [5].

A recent study has provided a comprehensive characterization of input redundancy in linear time-invariant (LTI) systems [2]. The approach relies on geometric control theory tools [6], particularly controlled-invariant and output-invisible subspaces, which are central to the understanding of input redundancy. Controlled-invariant subspaces can be kept invariant using appropriate control inputs, meaning the state of the system remains within these subspaces once entered inside. This is achieved through state feedback, commonly referred to as a *friend* of the subspace, which plays a crucial role in the analysis and design of input redundant systems.

While input redundancy provides significant benefits, adding extra inputs also increases the complexity of system analysis and control. Identifying which inputs are redundant becomes essential for reducing complexity and improving system efficiency, especially in large-scale systems like batteries, multicell converters, and supercapacitor systems [7], [8], [9]. In such cases, applying the characterization from [2], however, presents significant computational challenges. In particular, the computation of the controlled-invariant, output-invisible subspaces, and the friend necessary for state feedback, not only demands significant time and computational resources but is also prone to numerical inaccuracy. The latter is due to inevitable finite-precision arithmetic, subspace computation sensitivities, and loss of numerical rank [10]. As a result, some inputs are incorrectly identified as 'invisible' when they are not, leading to inevitable performance degradation and potentially harming the system.

In this context, this article aims to analyze input redundancy in large-scale systems using model order reduction techniques. Among the multitude of reduction techniques, we focus here on balanced truncation [11]. Balanced truncation operates by first bringing the system in a so-called balanced form in which the transformed states are ordered in terms of their controllability and observability. Then, by retaining only the most controllable and observable states, a reduced-order model is constructed that closely approximates the original system. This reduced model, easier to manipulate, is key to identifying redundant inputs, as it preserves the essential dynamics of the system while simplifying its state space representation. Based on the reduced-order model, we compute the friend state feedback so that specific inputs do not influence the output of the closed-loop reduced-order model. Once these inputs are identified, we apply them to the original system, as feedforward inputs. Through a careful error analysis based on the well-known balanced truncation error bound, we demonstrate that these inputs yield an almost zero output in the original system and are thus *almost invisible* to the original system. This leads to a novel control architecture that decouples the visible inputs from the almost invisible ones.

This novel combination of balanced truncation and the state-feedback friend offers a powerful framework for input redundancy analysis. By utilizing the reduced-order model to determine redundant inputs and analyzing their effect on the original system, we provide a systematic approach to simplifying complex systems while maintaining their core functionality. Our results offer significant computational savings and open new avenues for designing and controlling more efficient and more robust input-redundant systems.

The rest of this article is organized as follows. Section II introduces preliminaries on input redundant systems and defines the problem addressed in this article. Section III presents the proposed approach based on model reduction by balanced truncation. In Section IV, we present numerical examples to demonstrate the effectiveness of our approach. Finally, Section V closes with concluding remarks.

Notation: The symbols $\mathbb{R}, \mathbb{R}^+, \mathbb{C}$, and $\mathbb{C}^-$ denote the sets

J. Kreiss and M. Jungers are with Université de Lorraine, CNRS, CRAN, 54000 Nancy, France ([jeremie.kreiss;marc.jungers]@univ-lorraine.fr)

M.F. Shakib is with the Department of Electrical and Electronic Engineering, Imperial College London, London, UK (m.shakib@imperial.ac.uk)

This work has been partially supported by the Engineering and Physical Sciences Research Council, Grant EP/X033546/1.

of real numbers, non-negative real numbers, complex numbers, and complex numbers with strictly negative real parts, respectively. A square real-valued matrix is called Hurwitz if all its eigenvalues have a strictly negative real part. The class $L_2^m(\mathcal{T})$ represents the class of functions $x : \mathcal{T} \to \mathbb{R}^m$ for some $\mathcal{T} \subseteq \mathbb{R}$ which are bounded as $\int_{\mathcal{T}} |x(t)|^2 \mathrm{d}t < \infty$. The corresponding L_2^m signal norm is denoted by $\|x\|_2$ and defined by $\|x\|_2^2 \coloneqq \int_{\mathcal{T}} |x(t)|^2 \mathrm{d}t$. For a transfer-function matrix G defined on $\mathbb{C}$, with all its poles in $\mathbb{C}^-$, its $\mathcal{H}_\infty$-norm is defined by $\|G\|_{\mathcal{H}_\infty} \coloneqq \sup_{\omega \in [0,\infty)} \bar{\rho}(G(j\omega))$ with $\bar{\rho}$ the maximum singular value of G and $j \coloneqq \sqrt{-1}$. Given a set $\mathcal{S} \subseteq \mathbb{R}^n$ and a real-valued matrix $B \in \mathbb{R}^{n \times m}$, the set $B^{-1}\mathcal{S}$ is defined as $\{u \in \mathbb{R}^m : Bu \in \mathcal{S}\}$.

II. Problem statement

This section first reviews key concepts from geometric control theory and the property of input redundancy. We then explain how we can decouple input trajectories in output visible and invisible ones for IR systems. Finally, we outline the specific problem addressed in this article. Throughout this article, we consider the LTI system Σ governed by the following equations:

$$\dot{x} = Ax + Bu,\ x(0) \coloneqq x_0 \in \mathbb{R}^n, \tag{1a}$$

$$y = Cx + Du, \tag{1b}$$

where A, B, C, and D are matrices of appropriate dimensions. Here, $u : \mathbb{R}^+ \to \mathbb{R}^m$, $x : \mathbb{R}^+ \to \mathbb{R}^n$, and $y : \mathbb{R}^+ \to \mathbb{R}^p$ represent the input, the state, and the output, respectively.

A. Background on geometric control theory

To analyze the input redundancy property of a system, we introduce some key concepts from geometric control theory. A subspace $\mathcal{V} \subseteq \mathbb{R}^n$ is called *controlled-invariant and output-invisible* if it satisfies the following conditions:

$$A\mathcal{V} \subseteq \mathcal{V} + \mathrm{Im}\{B\},\ C\mathcal{V} \subseteq \mathrm{Im}\{D\},$$

or equivalently, if there exists a matrix $F \in \mathbb{R}^{m \times n}$ such that

$$(A + BF)\mathcal{V} \subseteq \mathcal{V},\ (C + DF)\mathcal{V} = 0.$$

Such a matrix F is referred to as a *friend* of $\mathcal{V}$. Note that in general, a subspace $\mathcal{V}$ does not have a unique friend. The set of friends of $\mathcal{V}$ is denoted by $\mathbb{F}(\mathcal{V})$.

The subspace $\mathcal{V}^*$, known as the *weakly unobservable subspace*, is the largest *controlled-invariant and output-invisible* subspace of Σ. It represents the set of initial conditions $x_0 \in \mathbb{R}^n$ for which there exists an input $u : \mathbb{R}^+ \to \mathbb{R}^n$ such that $\forall t \in \mathbb{R}^+$, $x(t) \in \mathcal{V}^*$ and $y(t) = 0$. Note that this subspace can be computed in a finite number of steps using only the system matrices A, B, C, and D (see [6, Th. 7.12]). The subspace $\mathcal{R}^*$ called the *controllable weakly unobservable subspace*, corresponds to the largest controllable subspace within $\mathcal{V}^*$.

B. The notion of input redundancy

We now recall the definition of input redundancy as presented in [2].

Definition 1: System Σ is said to be *input redundant* (IR) if there exists an output y which can be produced by (at least) two distinct inputs for some $x_0 \in \mathbb{R}^n$, i.e., there exists $x_0 \in \mathbb{R}^n$ such that

$$\exists (u_1, y_1), (u_2, y_2) : u_1 \neq u_2, y_1 = y_2. \tag{2}$$

It is important to note that in the context of LTI systems, the input redundancy property is uniform with respect to the initial condition. That is, if there exists an initial condition $x_0 \in \mathbb{R}^n$ such that condition (2) holds, then it holds for all $x_0 \in \mathbb{R}^n$. Therefore the input redundancy property can be derived to the quadruple (A, B, C, D) in the following way: the system defined by the matrices A, B, C, and D is considered IR if, for any initial condition $x_0 \in \mathbb{R}^n$, the system exhibits input redundancy.

Next, we recall the geometric characterization of Definition 1, summarized in the following theorem [2, Th. 3.1].

Theorem 1: Let $\mathcal{N} \coloneqq B^{-1}\mathcal{V}^* \cap \mathrm{Ker}\{D\}$ be an input subspace and define μ as its dimension, i.e., $\mu \coloneqq \dim \mathcal{N}$. The following statements are equivalent:

- Σ is IR;
- $\dim \mathcal{N} > 0$. □

It is emphasized that, unlike earlier characterizations of this concept [1], the input redundancy characterization here is not solely based on the kernel of B and D. Instead, it relies on deeper geometric properties that involve the underlying structure of the input-to-output map of the system.

C. Input decomposition

For LTI systems (1), as shown in [6, Th. 7.11], the output resulting from an input u and an initial condition x_0 is zero if and only if $x_0 \in \mathcal{V}^*$ and the input u is given by

$$u = Fx + \hat{L}\hat{v}, \tag{3}$$

where $F \in \mathbb{F}(\mathcal{V}^*)$, $\hat{L} \in \mathbb{R}^{m \times \mu}$ is a linear map such that $\mathrm{Im}\left\{\hat{L}\right\} = \mathcal{N}$, and $\hat{v} : \mathbb{R}^+ \to \mathbb{R}^\mu$ is any arbitrary function. In line with the definition of IR systems, we are interested in different inputs that lead to the same output, starting from the same initial condition. An incremental analysis can demonstrate that this problem can be reduced to the existence of invisible inputs, starting with the zero initial condition $x_0 = 0$. Since $\mathcal{V}^*$ is a subspace of $\mathbb{R}^n$, it follows that $x_0 = 0 \in \mathcal{V}^*$ and we are typically concerned with *invisible inputs* whose expression is given by (3).

For IR systems, it is evident that $\mu > 0$ implies that the matrix $\hat{L}$ is non-empty and non-zero. Therefore, it is always possible to construct non-zero inputs that result in zero outputs. We define $\tilde{L} \in \mathbb{R}^{n \times (m-\mu)}$ such that $\mathrm{Im}\left\{\begin{bmatrix}\hat{L} & \tilde{L}\end{bmatrix}\right\} = \mathbb{R}^m$, thereby completing the input space. This allows us to isolate the component $\tilde{v}$ of the input that has an actual influence on the output y through the matrix $\tilde{L}$. Thus, we decompose the inputs into $\hat{v}$ which has no effect on the output, and $\tilde{v}$ which has a direct effect. The corresponding

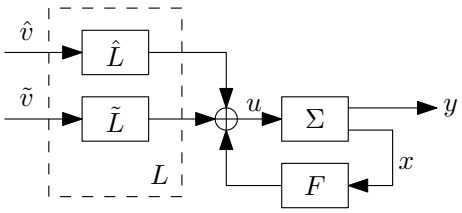

Fig. 1: Input decomposition scheme with control law (4).

scheme is depicted in Figure 1. The state feedback law with the decomposed inputs is then described by

$$u = Fx + Lv, \tag{4}$$

where $L := \begin{bmatrix}\hat{L} & \tilde{L}\end{bmatrix} \in \mathbb{R}^{n\times m}$, $v := \begin{bmatrix}\hat{v}^\top & \tilde{v}^\top\end{bmatrix}^\top$, and $\hat{v}$ is invisible for the output y.

D. Problem formulation

The input decomposition discussed in the previous section is highly valuable in many control [1], fault-detection [12], and fault-tolerance [13] applications. However, it relies on knowledge of $\mathcal{V}^*$, F, and $\mathcal{N}$, which can be challenging to compute numerically for large-scale systems, both in terms of computation time and accuracy. In particular, computational inaccuracies combined with modeling uncertainties can distort the feedback law (3), potentially leading to non-zero output trajectories even if $\tilde{v} = 0$.

To illustrate these computational challenges, we generate random systems (1) with parameters $m = 3$, $p = 1$, and n varying from 20 to 400 with increments of 20. The systems are generated using the MATLAB 2024a *rss* command. The elements $\mathcal{V}^*$, $\mathcal{N}$, and F are computed using MATLAB 2024a with the aid of the geometric control toolbox [14]. The corresponding computation times, denoted as $\Delta t_{\mathcal{V}^*}$, $\Delta t_{\mathcal{N}}$, and Δt_F, respectively, are plotted as a function of n in Figure 2. These results clearly demonstrate how the computation time scales with the state dimension n of the system.

In addition to the extensive computation times, accuracy issues may also arise when computing invisible inputs. For instance, consider a (Matlab 2024a *rss*) random system (1) with $m = 3$, $n = 200$, and $p = 1$. We apply an invisible input (3) where $\hat{v}(t) \in \mathbb{R}^2$ consists of block-wave signals with random magnitudes between -1 and 1. Both the input signal $\hat{v}$ and the resulting output y are shown in Figure 3. It is evident that the output is not zero. In fact, it exhibits a large magnitude (exceeding 50). This is mainly due to computational inaccuracies in computing the friend F and the matrix $\hat{L}$.

Given the numerical challenges and inherent modeling uncertainties, achieving strictly zero output with "invisible inputs" is often impractical. However, exact invisibility is rarely necessary in applications. Instead, achieving a small-gain energy transfer from input to the output can suffice to create *almost-invisible* inputs, as illustrated in control applications for power converters [15]. This need underscores the importance of a robust input decomposition method that achieves *almost-invisibility* without requiring the computation of $\mathcal{V}^*$, F, or $\mathcal{N}$. This article aims to address this challenge, focusing specifically on the following problem.

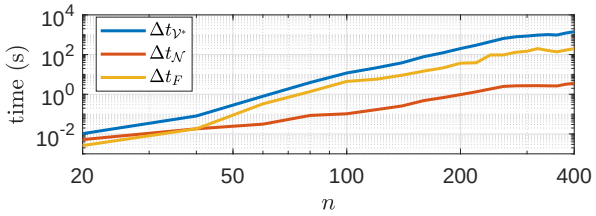

Fig. 2: Evolution of the computation time with respect to n on a log-log plot.

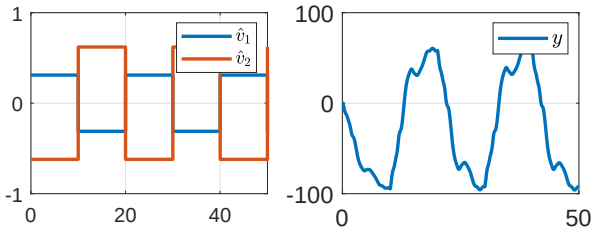

Fig. 3: Due to inaccurate computations, the "invisible" input $\hat{v} := \begin{bmatrix}\hat{v}_1^\top & \hat{v}_2^\top\end{bmatrix}^\top$ (left) results in a non-zero output (right).

Problem 1: For system Σ in (1), find a control architecture that can decouple inputs that are almost invisible from those that are visible in the output, without requiring the computation of $\mathcal{V}^*$, F, or $\mathcal{N}$ for system Σ.

III. A Control Architecture for Input Redundancy through Reduced-Order Modeling

This section proposes a control architecture that achieves *approximate* decoupling between visible and invisible inputs for input redundant systems. We first define the notion of *almost invisible inputs* in Section III-A. Then, we show in Section III-B how balanced truncation [11] can be used to characterize such inputs. By leveraging the error bounds of balanced truncation, we ensure that the decoupling achieved on the reduced-order model can be extended back to the *original* system, providing guarantees on its *approximate* decoupling properties. Finally, we propose a control architecture that approximately decouples the visible and invisible parts of the input for the original system in Section III-D.

A. δ-Almost invisible inputs

For IR systems, it is possible to perturb the input trajectory u without affecting the output trajectory y, i.e., $\exists(u, \delta u, y, \delta y) : u \neq u + \delta u, y = y + \delta y$. In some cases, however, achieving exactly $\delta y = 0$ is not required and a finite energy transfer is sufficient, i.e., a 'small' δy is sufficient. In this light, we define the notion of δ-almost invisible inputs.

Definition 2: For a given $\delta \in [0, \infty)$, an input $u \in L_2^m$ is *δ-almost invisible* for system Σ if the corresponding output y for the initial condition $x_0 = 0$ satisfies

$$\|y\|_2 \leq \delta \|u\|_2 . \tag{5}$$

The definition of a δ-almost invisible input is used in the remainder of this section to provide an input decoupling architecture that, for a perturbed input, produces almost the same output. This architecture is built based on reduced-order modeling as described next.

B. Reduced-order modeling through balanced truncation

We consider the scenario in which the system (1) is too complex for analysis (and control design). As a replacement for this system Σ, we consider the class of order r models Σ_r described by the equations

$$\dot{x}_r = A_r x_r + B_r u,\ x_r(0) \coloneqq x_{r,0}, \tag{6a}$$
$$y_r = C_r x_r + D_r u, \tag{6b}$$

where $r < n$, the matrices A_r, B_r, C_r, and D_r have appropriate dimensions, and $x_r : \mathbb{R}^+ \to \mathbb{R}^r$ is the state, $u : \mathbb{R}^+ \to \mathbb{R}^m$ is the input, and $y_r : \mathbb{R}^+ \to \mathbb{R}^p$ is the output.

We consider model reduction by balanced truncation to obtain the reduced-order model (6) from the original system (1). Balanced truncation is a two-step procedure [11]. In the first step, the system is brought into a balanced form. Let $P \in \mathbb{R}^{n\times n}$ and $Q \in \mathbb{R}^{n\times n}$ be the solutions to the following Lyapunov equations

$$AP + PA^\top + BB^\top = 0,\ A^\top Q + QA + C^\top C = 0, \tag{7}$$

respectively, where P and Q are called the controllability and observability Gramians, respectively. Under the assumption that A is Hurwitz, the pair (A, B) is controllable, and the pair (A, C) is observable, the solutions P and Q are unique, symmetric, and positive-definite matrices. Applying a Cholesky factorization on Q and P, we write $Q = \tilde{Q}\tilde{Q}^\top$ and $P = \tilde{P}\tilde{P}^\top$, where $\tilde{Q}$ and $\tilde{P}$ are invertible matrices. Let $Z\Psi Y^\top$ be the singular value decomposition of $\tilde{P}^\top\tilde{Q}$, i.e., $\tilde{P}^\top\tilde{Q} = Z\Psi Y^\top$ with $\Psi = \operatorname{diag}\left\{\sigma_1 I_{m_1}, \sigma_2 I_{m_2}, \ldots, \sigma_q I_{m_q}\right\}$, where $\sigma_i, i \in \{1, \ldots, q\}$, are the Hankel singular values of system Σ, and Z and Y are unitary matrices. Suppose that the Hankel singular values satisfy the ordering $\sigma_1 > \sigma_2 > \cdots > \sigma_q > 0$ and their multiplicities $m_i, i \in \{1, \ldots, q\}$, add up to n, i.e., $m_1 + \cdots + m_q = n$. Then, the matrices of a balanced realization of system Σ are given by

$$\left[\begin{array}{c|c} T^{-1}AT & T^{-1}B \\ \hline CT & D \end{array}\right], \tag{8}$$

where $T^{-1} = \Psi^{-1/2}Y^\top\tilde{Q}^\top$ and $T = \tilde{P}Z\Psi^{-1/2}$.

To reduce the system, in the second step of balanced truncation, take the order r such that there exists an integer k that satisfies $m_1 + \cdots + m_k = r$. Then, we can use the following partitioning:

$$\left[\begin{array}{c|c} T^{-1}AT & T^{-1}B \\ \hline CT & D \end{array}\right] = \left[\begin{array}{cc|c} A_{11} & A_{12} & B_1 \\ A_{21} & A_{22} & B_2 \\ \hline C_1 & C_2 & D \end{array}\right], \tag{9}$$

in which $A_{11} \in \mathbb{R}^{r\times r}, A_{12} \in \mathbb{R}^{r\times(n-r)}, A_{21} \in \mathbb{R}^{(n-r)\times r}, A_{22} \in \mathbb{R}^{(n-r)\times(n-r)}, B_1 \in \mathbb{R}^{r\times m}, B_2 \in \mathbb{R}^{(n-r)\times m}, C_1 \in \mathbb{R}^{p\times r}$, and $C_2 \in \mathbb{R}^{p\times(n-r)}$. Now, the matrices of the reduced-order model (6) are defined by truncating the matrices in (9), leading to

$$\left[\begin{array}{c|c} A_r & B_r \\ \hline C_r & D_r \end{array}\right] \coloneqq \left[\begin{array}{c|c} A_{11} & B_1 \\ \hline C_1 & D \end{array}\right]. \tag{10}$$

It is well-known that the transfer function of the model (6) with the matrices (10) does not achieve a match at 0 with the transfer function of the original system (1). To obtain such a match, the matrices of the reduced-order model (6) are selected according to the singular perturbation approach [16]:

$$\left[\begin{array}{c|c} A_r & B_r \\ \hline C_r & D_r \end{array}\right] \coloneqq \left[\begin{array}{c|c} A_{11} - A_{12}A_{22}^{-1}A_{21} & B_1 - A_{12}A_{22}^{-1}B_2 \\ \hline C_1 - C_2A_{22}^{-1}A_{21} & D - C_2A_{22}^{-1}B_2 \end{array}\right]. \tag{11}$$

The reduced-order model (6) with matrices (11) matches the steady-state gain of the original system. We refer to the reduced-order model (6) obtained by balanced truncation if its matrices satisfy either (10) or (11). In both cases, such a reduced-order model enjoys several properties, which are recalled next.

Theorem 2 ([17, Theorems 2.8 and 2.9]): Let system (1) be asymptotically stable and in a balanced realization, and let (6) be a reduced-order model obtained by balanced truncation. Assume that r is chosen such that there exists an integer k satisfying $m_1 + \cdots + m_k = r$. Then, the model (6) is balanced and asymptotically stable. Furthermore, the bound

$$\|\Sigma - \Sigma_r\|_{\mathcal{H}_\infty} \leq 2\left(\sigma_{k+1} + \cdots + \sigma_q\right) =: \varepsilon_r, \tag{12}$$

holds, where $\sigma_{k+1}, \ldots, \sigma_q$, can be read off the diagonal entries of the matrix Ψ. □

Balanced truncation thus preserves asymptotic stability and is equipped with the error bound (12). This error bound implies a time-domain error bound, i.e., for the initial conditions $x_0 = x_{r,0} = 0$, and any input $u \in L_2^m$, the bound

$$\|y - y_r\|_2 \leq \varepsilon_r \|u\|_2, \tag{13}$$

holds, where y and y_r are corresponding responses of the system (1) and of the reduced-order model (6), see, e.g., [18]. Based on this error bound, we establish a set of δ-almost invisible inputs for system (1) in the next section.

C. Invisible inputs for the reduced-order model

Let us assume that r is sufficiently small to efficiently and accurately compute $\mathcal{V}_r^*$, F_r, and $\mathcal{N}_r$ for the reduced-order model (6), and suppose that $\mu_r \coloneqq \dim \mathcal{N}_r > 0$. Furthermore, let the decoupling matrix $L_r \in \mathbb{R}^{m\times m}$ play the role of L. Then, similar to (4), the input can be decomposed into a part that is invisible to the output and a part that affects the output. Let us decompose the matrix L_r and the input v as follows:

$$L_r = \begin{bmatrix}\hat{L}_r & \tilde{L}_r\end{bmatrix}, \qquad v = \begin{bmatrix}\hat{v}^\top & \tilde{v}^\top\end{bmatrix}^\top, \tag{14}$$

where $\hat{L}_r \in \mathbb{R}^{m\times\mu_r}$, $\tilde{L}_r \in \mathbb{R}^{m\times(m-\mu_r)}$, $\hat{v}(t) \in \mathbb{R}^{\mu_r}$, and $\tilde{v}(t) \in \mathbb{R}^{m-\mu_r}$. Then, any input $\hat{v} \in L_2^{\mu_r}$, $\tilde{v} = 0$ is invisible for the reduced-order model (6), i.e., $y_r = 0$.

We now present a result in which we bound the signal u in the scheme in Figure 4. Hereto, note that the transfer function from v to u can be written as

$$G_{uv}(s) \coloneqq (I - F_r(sI - A_r)^{-1}B_r)^{-1}L_r, \quad s \in \mathbb{C}, \tag{15}$$

whereas the transfer function from $\hat{v}$ to u reads as follows:

$$G_{u\hat{v}}(s) \coloneqq (I - F_r(sI - A_r)^{-1}B_r)^{-1}\hat{L}_r, \quad s \in \mathbb{C}. \tag{16}$$

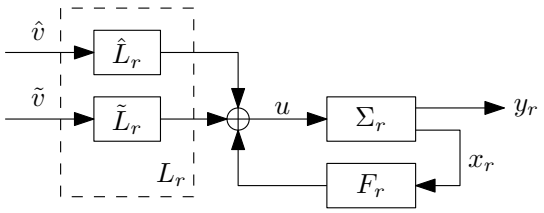

Fig. 4: Input decoupling for the reduced-order model (6).

Lemma 3: Consider the model Σ_r in (6), a friend F_r, the decoupling matrix matrix L_r, and the feedback law $u = F_r x_r + L_r v$. Suppose that $A_r + B_r F_r$ is Hurwitz. Then, for any bounded input $v \in L_2^m$ and the initial condition $x_{r,0} = 0$, the signal u is in L_2^m and satisfies

$$\|u\|_2 \leq \underbrace{\|G_{uv}(s)\|_{\mathcal{H}_\infty}}_{=:\gamma_u} \|v\|_2 , \tag{17}$$

where $\gamma_u \in [0, \infty)$. Furthermore, consider the decomposition (14). Then, for any $\hat{v} \in L_2^{\mu_r}$, $\tilde{v} = 0$, and the initial condition $x_{r,0} = 0$, the signal u is in L_2^m and satisfies

$$\|u\|_2 \leq \underbrace{\|G_{u\hat{v}}(s)\|_{\mathcal{H}_\infty}}_{=:\hat{\gamma}_u} \|v\|_2 , \tag{18}$$

where $\hat{\gamma}_u \in [0, \gamma_u]$. □

We note that, in general, neither γ_u nor $\hat{\gamma}_u$ are small valued, even if the reduced-order model is input redundant. This leads to the input u to the reduced-order model being generally not small in L_2^m-norm.

D. δ-Almost invisible inputs for the original system

While any input $\hat{v} \in L_2^{\mu_r}$, $\tilde{v} = 0$ result in $y_r = 0$, applying the corresponding input u to the original system Σ does not necessarily result in $y = 0$, but rather in a non-zero trajectory for y. In this section, we derive a bound for the L_2^p-norm of y.

To solve Problem 1, we propose the architecture depicted in Figure 5. Here, the input v is decoupled based on the reduced-order model, similar to the architecture in Figure 4. Then, the input u is applied to the system Σ. The state-space description of this interconnection is described by:

$$\begin{bmatrix} \dot{x}_r \\ \dot{x} \end{bmatrix} = \begin{bmatrix} A_r + B_r F_r & 0 \\ BF_r & A \end{bmatrix} \begin{bmatrix} x_r \\ x \end{bmatrix} + \begin{bmatrix} B_r \\ B \end{bmatrix} L_r \begin{bmatrix} \hat{v} \\ \tilde{v} \end{bmatrix}, \tag{19a}$$

$$y = \begin{bmatrix} DF_r & C \end{bmatrix} \begin{bmatrix} x_r \\ x \end{bmatrix} + DL_r \begin{bmatrix} \hat{v} \\ \tilde{v} \end{bmatrix}, \tag{19b}$$

where $v(t) \in \mathbb{R}^m$, $\begin{bmatrix} x_r^\top(t) & x^\top(t) \end{bmatrix}^\top \in \mathbb{R}^{n+r}$, and $y(t) \in \mathbb{R}^p$ are the input, the state, and the output at time t, respectively.

We analyze δ-almost invisible inputs for system Σ in (1) next. The main result of this article presents a bound for the output y of the original system Σ in (1) and characterizes a set of δ-almost invisible inputs $\mathcal{U}_\delta$, *without* computing $\mathcal{V}^*$, F, or $\mathcal{N}$ of the original system Σ.

Theorem 4: Consider the setting of Lemma 3, where Σ_r in (6) is obtained through balanced truncation from the system Σ in (1). Consider the interconnected system (19) and suppose that A and $A_r + B_r F_r$ are Hurwitz matrices. Then,

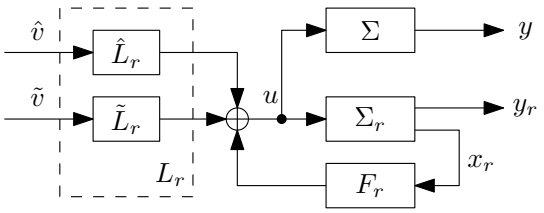

Fig. 5: Decoupling of the visible and the δ-almost invisible inputs for the original system based on the interconnection structure (19).

for any bounded input $v \in L_2^m$ and the initial conditions $x_{r,0} = x_0 = 0$, the signal y is in L_2^p and satisfies

$$\|y - y_r\|_2 \leq \varepsilon_r \gamma_u \|v\|_2 , \tag{20}$$

where $\gamma_u \in [0, \infty)$ is defined in Lemma 3 and $\varepsilon_r \in [0, \infty)$ is defined in (12). Furthermore, for any $\hat{v} \in L_2^{\mu_r}$, $\tilde{v} = 0$, and the initial conditions $x_{r,0} = x_0 = 0$, the signal y is in L_2^p and satisfies

$$\|y\|_2 \leq \delta_r \|v\|_2 , \tag{21}$$

where δ_r is defined as

$$\delta_r := \left\| \left(C(sI_n - A)^{-1} B + D \right) G_{u\hat{v}}(s) \right\|_{\mathcal{H}_\infty} \tag{22}$$

and satisfies $\delta_r \leq \varepsilon_r \hat{\gamma}_u$ and $\hat{G}_{uv}(s)$ is as defined in (16). Finally, any input u from the set

$$\mathcal{U}_\delta := \{ v \in L_2^m : \hat{v} \in L_2^{\mu_r}, \tilde{v} = 0 \}, \tag{23}$$

is δ_r-almost invisible for system Σ in (1) with δ_r in (22). □

Theorem 4 shows that, for any input from the set $\mathcal{U}_\delta$, the output y of the *original* system remains close to zero with a computable bound. Thereby, the architecture in Figure 5 solves Problem 1. In this architecture, the input $\tilde{v}$ is used for a primary task such as regulation, while the δ-almost invisible input $\hat{v}$ is used for a secondary task such as control allocation and fault detection.

We care to stress that the architecture in Figure 5 is achieved by only performing computations on the matrices of the *reduced-order model*. This enables the application of IR tools to large-scale systems. In the next section, we demonstrate the performance of the proposed architecture in Figure 5 using numerical examples.

Remark 1: The results of Lemma 3 and Theorem 4 require $A_r + B_r F_r$ to be Hurwitz. If the reduced-order model is IR and A_r is Hurwitz, then there exists a friend $F_r \in \mathbb{F}(\mathcal{R}_r^*)$ (where $\mathcal{R}_r^*$ is the controllable weakly unobservable subspace of Σ_r) that ensures $A_r + B_r F_r$ is Hurwitz, see [6, Th. 4.18].

Remark 2: Unlike the architecture in Figure 1, the architecture in Figure 5 operates without requiring knowledge of the system state x of the original system Σ. In large-scale systems, state estimation via an observer is challenging due to the high state dimension and the computational limitations of resource-constrained devices. By eliminating the need for direct state estimation, the architecture in Figure 5 facilitates real-time operation in such scenarios.

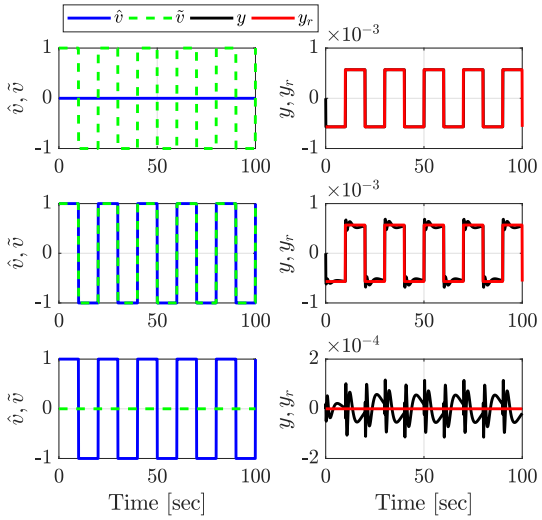

Fig. 6: Time-domain simulations for the full-order system and the reduced-order model. Each row corresponds to a simulation with the applied input depicted in the left column and the corresponding system response y and reduced-order model response y_r depicted in the right column.

IV. Numerical example

We consider the so-called heat equation in a thin rod benchmark system given in [19]. The benchmark system is of order $n = 200$ and is a single-input, single-output system. To make it an IR system, we augment the matrix B with a column with random numbers such that the system is input redundant. We drastically reduce this system to order $r = 5$ using balanced truncation with the relations (11). Then, for the reduced-order model, we compute F_r and L_r, and we implement the architecture in Figure 5.

We perform three simulations with block-wave inputs as depicted in Figure 6 and with zero initial conditions. For the first simulation (top row of Figure 6), $\tilde{v}$ is a block-wave signal whereas $\hat{v} = 0$. For the second one (middle row of Figure 6), both $\tilde{v}$ and $\hat{v}$ are block-wave signals (with the same amplitude, frequency, and phase). In the third simulation (bottom row of Figure 6), $\tilde{v} = 0$ and $\hat{v}$ is a block-wave signal. We observe from Figure 6 that the inputs $\hat{v}$, which are invisible for the reduced-order model, are *δ-almost invisible* for the original system. Here, we emphasize that we reduced the system order drastically, allowing for the efficient analysis and design of the friend F_r, the decoupling matrix L_r, and auxiliary subspaces. For the original system, the required matrices for input decoupling can be computed within *minutes*, while this is a matter of *seconds* using the reduced-order matrices. Such a drastic reduction of the state order also enables the efficient online implementation of the scheme in Figure 5 on devices with limited resources, see Remark 2.

V. Conclusions

This article presents a control architecture for large-scale input redundant systems using model reduction by balanced truncation. The architecture facilitates the decoupling of visible and almost invisible inputs, where *δ-almost invisible* inputs for the original system are characterized through the application of the error bound of balanced truncation. The proposed approach thus enables the analysis and design of complex input redundant systems and is also an enabler for supporting applications such as control allocation and fault detection. Future research will explore extensions to the taxonomy-preservation of input redundancy through model reduction and practical applications.

References

[1] T. A. Johansen and T. I. Fossen, "Control allocation—A survey," *Automatica*, vol. 49, no. 5, pp. 1087–1103, 2013.

[2] J. Kreiss and J.-F. Trégouët, "Input redundancy: Definitions, taxonomy, characterizations and application to over-actuated systems," *Systems & Control Letters*, vol. 158, p. 105060, 2021.

[3] J.-F. Trégouët, D. Arzelier, D. Peaucelle, C. Pittet, and L. Zaccarian, "Reaction Wheels Desaturation Using Magnetorquers and Static Input Allocation," *IEEE Transactions on Control Systems Technology*, vol. 23, no. 2, pp. 525–539, 2015.

[4] Y. Huang and C. K. Tse, "Circuit Theoretic Classification of Parallel Connected DC/DC Converters," *IEEE Transactions on Circuits and Systems I: Regular Papers*, vol. 54, no. 5, pp. 1099–1108, 2007.

[5] J. Kreiss, M. Bodson, R. Delpoux, J.-Y. Gauthier, J.-F. Trégouët, and X. Lin-Shi, "Optimal control allocation for the parallel interconnection of buck converters," *Control Engineering Practice*, vol. 109, p. 104727, 2021.

[6] H. L. Trentelman, A. A. Stoorvogel, and M. Hautus, *Control Theory for Linear Systems*. Communications and Control Engineering, Springer London, 2001.

[7] W. Huang and J. A. Abu Qahouq, "Energy Sharing Control Scheme for State-of-Charge Balancing of Distributed Battery Energy Storage System," *IEEE Transactions on Industrial Electronics*, vol. 62, no. 5, pp. 2764–2776, 2015.

[8] D. Linzen, S. Buller, E. Karden, and R. De Doncker, "Analysis and evaluation of charge-balancing circuits on performance, reliability, and lifetime of supercapacitor systems," *IEEE Transactions on Industry Applications*, vol. 41, no. 5, pp. 1135–1141, 2005.

[9] G. L. Goff, M. Fadel, and M. Bodson, "Scalable Optimal Control Allocation: Linear and Quadratic Programming Methods Applied to Active Capacitor Balancing in Modular Multilevel Converters," *IFAC-PapersOnLine*, vol. 55, no. 16, pp. 80–85, 2022.

[10] N. J. Higham and T. Mary, "Mixed precision algorithms in numerical linear algebra," *Acta Numerica*, vol. 31, pp. 347–414, 2022.

[11] B. Moore, "Principal component analysis in linear systems: Controllability, observability, and model reduction," *IEEE Transactions on Automatic Control*, vol. 26, no. 1, pp. 17–32, 1981.

[12] F. Cao, Z. Zhang, and X. He, "Active fault isolation of over-actuated systems based on a control allocation approach," *IEEE Transactions on Instrumentation and Measurement*, vol. 71, pp. 1–10, 2022.

[13] A. Casavola and E. Garone, "Fault-tolerant adaptive control allocation schemes for overactuated systems," *International journal of robust and nonlinear control*, vol. 20, no. 17, pp. 1958–1980, 2010.

[14] G. Marro, "The geometric approach tools," *Available from the web page: http://www3. deis. unibo. it/Staff/FullProf/GiovanniMarro/downloads. htm*, 2004.

[15] J. Kreiss, J.-F. Trégouët, D. Eberard, R. Delpoux, J.-Y. Gauthier, and X. Lin-Shi, "Hamiltonian Point of View on Parallel Interconnection of Buck Converters," *IEEE Transactions on Control Systems Technology*, vol. 29, no. 1, pp. 43–52, 2021.

[16] K. Fernando and H. Nicholson, "Singular perturbational model reduction of balanced systems," *IEEE Transactions on Automatic Control*, vol. 27, no. 2, pp. 466–468, 1982.

[17] B. Besselink, N. van de Wouw, and H. Nijmeijer, "Model reduction for a class of convergent nonlinear systems," *IEEE Transactions on Automatic Control*, vol. 57, no. 4, pp. 1071–1076, 2011.

[18] N. Kottenstette, M. J. McCourt, M. Xia, V. Gupta, and P. J. Antsaklis, "On relationships among passivity, positive realness, and dissipativity in linear systems," *Automatica*, vol. 50, no. 4, pp. 1003–1016, 2014.

[19] Y. Chahlaoui and P. Van Dooren, "A collection of benchmark examples for model reduction of linear time invariant dynamical systems.," 2002. Available at: `https://www.slicot.org/objects/software/reports/SLWN2002-2.ps.gz`.